

Received: 2020.01.06

Accepted: 2020.04.19

Available online: 2020.06.17

Published: 2020.08.16

***Ginkgo biloba* Extract EGb761 Attenuates Bleomycin-Induced Experimental Pulmonary Fibrosis in Mice by Regulating the Balance of M1/M2 Macrophages and Nuclear Factor Kappa B (NF-κB)-Mediated Cellular Apoptosis**

Authors' Contribution:

Study Design A
Data Collection B
Statistical Analysis C
Data Interpretation D
Manuscript Preparation E
Literature Search F
Funds Collection G

AD **Ling Pan**
BCE **Yuehong Lu**
BCEF **Zhanhua Li**
BF **Yuping Tan**
BF **Hongmei Yang**
CDF **Ping Ruan**
BF **Ruixiang Li**

Respiratory Medicine Department, Ruikang Hospital Affiliated to Guangxi Traditional Chinese Medicine University, Nanning, Guangxi, P.R. China

Corresponding Author: Ling Pan, e-mail: lingpandoc@aliyun.com

Source of support: Departmental sources

Background: The aim of this study was to show whether the standardized *Ginkgo biloba* extract EGb761, a traditional Chinese medicine, has a therapeutic effect on pulmonary fibrosis (PF).


Material/Methods: Bleomycin (BLM) was used for establishing the PF mouse model. The mice were treated with a gradient of EGb761 for 28 days to determine an appropriate drug dose. On day 28, the effect of EGb761 on lung injury and inflammation was confirmed by hematoxylin and eosin and Masson staining and evaluated by pulmonary alveolitis and Ashcroft score. The balance of M1/M2 macrophages was evaluated with the respective markers inducible nitric oxide synthase and interleukin-10 by real-time polymerase chain reaction. Furthermore, the expressions of fibrosis-associated protein α -smooth muscle actin (SMA), related inflammatory protein transforming growth factor (TGF)- β 1, the apoptosis-related proteins B-cell lymphoma-associated X protein (Bax), B-cell lymphoma (Bcl)-2, caspase-3, caspase-9, and phosphorylated nuclear factor (NF)- κ B (p65) were assessed by western blot.

Results: On day 28, PF was induced by treating with BLM, whereas EGb761 suppressed the PF of lung tissue. The BLM-induced imbalance of M1/M2 macrophages was reduced by EGb761. Furthermore, the increasing amounts of α -SMA and TGF- β 1 induced by BLM were suppressed by EGb761. In addition, the protein or messenger ribonucleic acid expression levels of phosphorylated NF- κ B (p65), caspase-3, and caspase-9 were upregulated, whereas Bax and Bcl-2 were downregulated. Treatment with EGb761 restored the levels of these proteins except for caspase-9.

Conclusions: This study illustrated the protective effect of EGb761 on BLM-induced PF by regulating the balance of M1/M2 macrophages and NF- κ B (p65)-mediated apoptosis. The results demonstrated the potential clinical therapeutic effect of EGb761, providing a novel possibility for curing PF.

MeSH Keywords: **Apoptosis • *Ginkgo biloba* • Idiopathic Pulmonary Fibrosis • Macrophages • Transcription Factor RelA**

Full-text PDF: <https://www.medscimonit.com/abstract/index/idArt/922634>

 2299

 1

 5

 59



Background

Pulmonary fibrosis (PF) is a chronic disease characterized by respiratory architecture injury and remodeling as well as heterogeneous fibroblast replacement [1,2]. The prevalence of PF is over 60 per 100 000 persons and has had a dramatic upward trend in recent years [3,4]. Much evidence reveals that idiopathic PF (IPF) has a poor prognosis; the overall survival rate of patients with IPF is no more than 5 years [5].

The pathogenesis of IPF is thought to have two causes. One is the unreversed extracellular matrix (ECM) sedimentation and lung chronic progressive inflammation. The other one is epithelial-to-mesenchymal transition (EMT) that has been revealed as a relevant contributor to IPF [6].

Macrophages are a type of immune cell involved in the pathogenesis of IPF via recruitment of other immune cells and secretion of proinflammatory cytokines to induce the proliferation and activation of collagen-secreting myofibroblasts [7–9]. Macrophages can functionally polarize into M1 or M2 forms during environmental changes [10]. M1 macrophages are activated in the initial inflammatory response, whereas M2 macrophages mediate tissue remodeling [11]. More important, M1/M2 macrophage polarization and the balance between M1 and M2 macrophages play a crucial role in the progression of fibrotic diseases [12,13]. Macrophages also generate reactive oxygen species (ROS) while initiating the immune response. The generated ROS induce the expression of transforming growth factor- β (TGF- β 1), which is an integral factor in fibrosis development via promotion of the EMT [14–17]. However, the increase in alveolar epithelial cell (AEC) apoptosis and the chronic and repetitive injury of AECs are implicated in the progression of IPF [18–21]. The gene expression profile of IPF patients has shown that the expression of epithelial proliferation and apoptosis-associated genes has increased [20]. Many studies support the hypothesis that apoptosis of AECs is the key factor in IPF [22–24].

The current pharmacological therapeutic approaches for PF involve treatment with corticosteroids, immunosuppressants, antifibrotic drugs, and cytotoxins [25,26], with no satisfactory result [27]. Therefore, developing or obtaining effective drugs for PF therapy remains a huge and pressing challenge. The standardized *Ginkgo biloba* extract EGb-761 is a traditional Chinese medicine. Like other traditional Chinese medicines, EGb-761 contains a variety of ingredients. Although the main active ingredient is not clear, EGb-761 has shown a neuroprotective effect on various neurological conditions such as brain stroke, Alzheimer's disease, and Parkinson's [28,29]. EGb761 shows its effects via inhibition of oxidative stress, apoptosis, and regulation of inflammatory responses [30–32]. Therefore, in this study, we use the PF mouse model to understand whether EGb761 has a therapeutic effect on PF.

Material and Methods

Experimental animals

Adult C57Bl6J mice weighing 20–25 g were available from the Ruikang Hospital Affiliated to Guangxi Traditional Chinese Medicine University. The mice were housed in a specific-pathogen-free facility and raised at a constant temperature of $25\pm 1^\circ\text{C}$ and an ambient noise of 40 ± 10 db. All the mice were freely fed for a 12-h light: dark cycle. Additionally, all the mice had free access to food and water. The care and use of experimental mice were approved by the Ethics Committee of Laboratory Animals of Guangxi Traditional Chinese Medicine University.

PF mouse model induction and bleomycin (BLM) treatment

The BLM-induced PF mouse model has similar inflammatory and fibrotic characteristics as human PF, and it is widely adopted to simulate the pathogenesis of PF [25,33]. The PF mouse model induced with BLM (MP Biomedicals, Shanghai, China) was performed as described before [33]. Briefly, 100 mice were randomly divided into five groups, with 20 animals per group: normal (untreated), BLM-treated group, and the EGb761-treated groups (low, medium, and high EGb761 dose). All mice were anesthetized intraperitoneally with 80 μL of a ketamine and xylazine solution (3.2 mg/kg and 0.169 mg/kg, respectively). For inducing PF, the mice were treated with an intratracheal instillation of 50 μL of BLM solution per day for 7 days. Meanwhile, the EGb761-treated groups were intraperitoneally injected with EGb761 (Guilin Technology Company Natural Plant Products, Guilin, China; 100 mg/kg, 50 mg/kg, and 25 mg/kg) once a day. The doses of EGb-761 were determined from previous studies [34–37]. The normal and EGb761-treated groups were intraperitoneally injected with an equal volume of saline once a day. Finally, all the mice were sacrificed on day 28 after model establishment and drug treatment.

Histologic detection and pulmonary fibrosis scoring

To determine the histopathologic changes of the lung tissues, the lung tissues of mice from each group were fixed and embedded, and then were stained with hematoxylin and eosin (H&E) and Masson stains and analyzed with Olympus Image Analysis system. H&E staining was used to reveal the alveolitis degree and Masson staining was applied to determine the collagen deposition and PF degree of the lung tissues. Pulmonary alveolitis and fibrosis were determined according to the criteria as previously reported [38,39].

Enzyme-linked immunosorbent assay (ELISA)

Mouse peripheral blood was collected on day 7 after BLM treatment. The levels of proinflammatory cytokines in serum,

including tumor necrosis factor (TNF)- β , interleukin (IL)-1 β , and IL-6, were detected by ELISA (ThermoFisher, Waltham, MA, USA). We followed the protocol of the kit.

Real-time polymerase chain reaction (RT-PCR)

Total ribonucleic acids (RNAs) were reverse transcribed into complementary deoxyribonucleic acid. The messenger (m)RNA expression levels of apoptosis factors as well as the markers of M1 and M2 macrophages were determined by RT quantitative (q)PCR following the SYBR-Green PCR master mix kit protocol (Applied Biosystems, Inc., Foster City, CA, USA). RT-qPCR was performed on an Applied Biosystems QuantStudio™6 Flex System. Primer sequences and the reference gene glyceraldehyde 3-phosphate dehydrogenase are shown in Table 1. The relative mRNA expression was measured with three independent experiments and calculated by the $2^{-\Delta\Delta Ct}$ method.

Western blot

Total protein samples were available from lysed lung tissues using sodium dodecyl sulfate (SDS; Beyotime, Shanghai, China) containing proteinase inhibitors and determined by bicinchoninic acid assay kit (Pierce Biotechnology, Inc., Rockford, IL, USA). SDS-polyacrylamide gel electrophoresis (10%) was applied to separate various protein bands, and all the bands were visible on polyvinylidene fluoride membranes (Millipore, Bedford, MA, USA). Then the membranes were incubated with primary antibodies anti-B-cell lymphoma-associated X protein (Bax), B-cell lymphoma (Bcl)-2, caspase-3, caspase-9 (1: 1000; Abcam, Cambridge, UK), and anti-tubulin (1: 1000, CST, Fall River, MA, USA) at 4°C overnight. Then the clean membranes were cocultured with horseradish peroxidase-conjugated goat anti-rabbit immunoglobulin G (Beyotime) for 2 h at room temperature. Finally, a specific band was enhanced with chemiluminescence reagent (ECL, Thermo) and was visible through the ChemiDoc MP system (Bio-Rad, Hercules, CA, USA)

Statistical analysis

Statistical analyses were carried out using the SPSS 21.0 software (IBM k, Armonk, NY, USA). All experimental data were shown as mean value \pm standard deviation. Differences between the two groups were determined by one-way analysis of variance. $P < 0.05$ was considered statistically significant.

Results

EGb761 reduced pulmonary inflammation induced by BLM in mice

After treating with BLM for 28 days, the level of inflammation in lung tissues was evaluated by the pulmonary alveolitis

Table 1. List of primer sequences used in real-time polymerase chain reaction.

Primers	Sequence (5'–3')
Bax-F	AAGAGCTGAGCGAGTGTCT
Bax-R	GTTCTGATCAGTCCGGCAC
Bcl-2-F	GCCTTCTTGAGTTCGGTGG
Bcl-2-R	CTCAGCCCAGACTCACATCA
Caspase-3-F	CAGCCAACCTCAGAGAGACA
Caspase-3-R	ACAGGCCCATTTGTCCATA
Caspase-9-F	CAGGACCTGGACAGTGACT
Caspase-9-R	AATGCCATCCAAGGTCTCGA
IL-10-F	GGTTGTCGTCTCATTCTGAAAGA
IL-10-R	GGTAGAGGACCCAAGTTCGTTAAGA
iNOS-F	CCCTTCAATGGTTGGTACATGG
iNOS-R	ACATTGATCTCCGTGACAGCC
GAPDH-F	CAACGGGAAACCCATCACCA
GAPDH-R	ACGCCAGTAGACTCCACGACAT

Bax – B-cell lymphoma-associated X protein; Bcl-2 – B-cell lymphoma-2; iNOS – inducible nitric oxide synthase; GAPDH – glyceraldehyde 3-phosphate dehydrogenase; F – forward; R – reverse.

score (Figure 1A). The pulmonary alveolitis score of the BLM-treated group showed the highest scores. In contrast, treatment with EGb761 significantly reduced the scores. The H&E staining showed that the pulmonary architecture was nearly destroyed and replaced in the BLM-treated group (Figure 1C) compared with the normal group (Figure 1B). However, treating with middle (Figure 1E) or high (Figure 1F) dose EGb761 rescued the destruction and replacement, which showed better effect than the low dose group (Figure 1D), manifested as less alveolar walls destruction and pulmonary architecture destruction. In addition, a size change of the airway, which may be caused by inflammation in the lung tissue, was observed.

EGb761 protects mice from PF induced by BLM

After being treated with BLM for 28 days, the fibrosis of lung tissues was observed by Masson staining and evaluated by the Ashcroft score (Figure 2). On day 28, the result of the Ashcroft score showed that the fibrosis level of lung tissue was significantly increased in the BLM-treated group compared with the normal group. However, the scores were reduced by treating with EGb761 (Figure 2A). In addition, large amounts of collagen accumulation and deposition in the areas of lung parenchyma

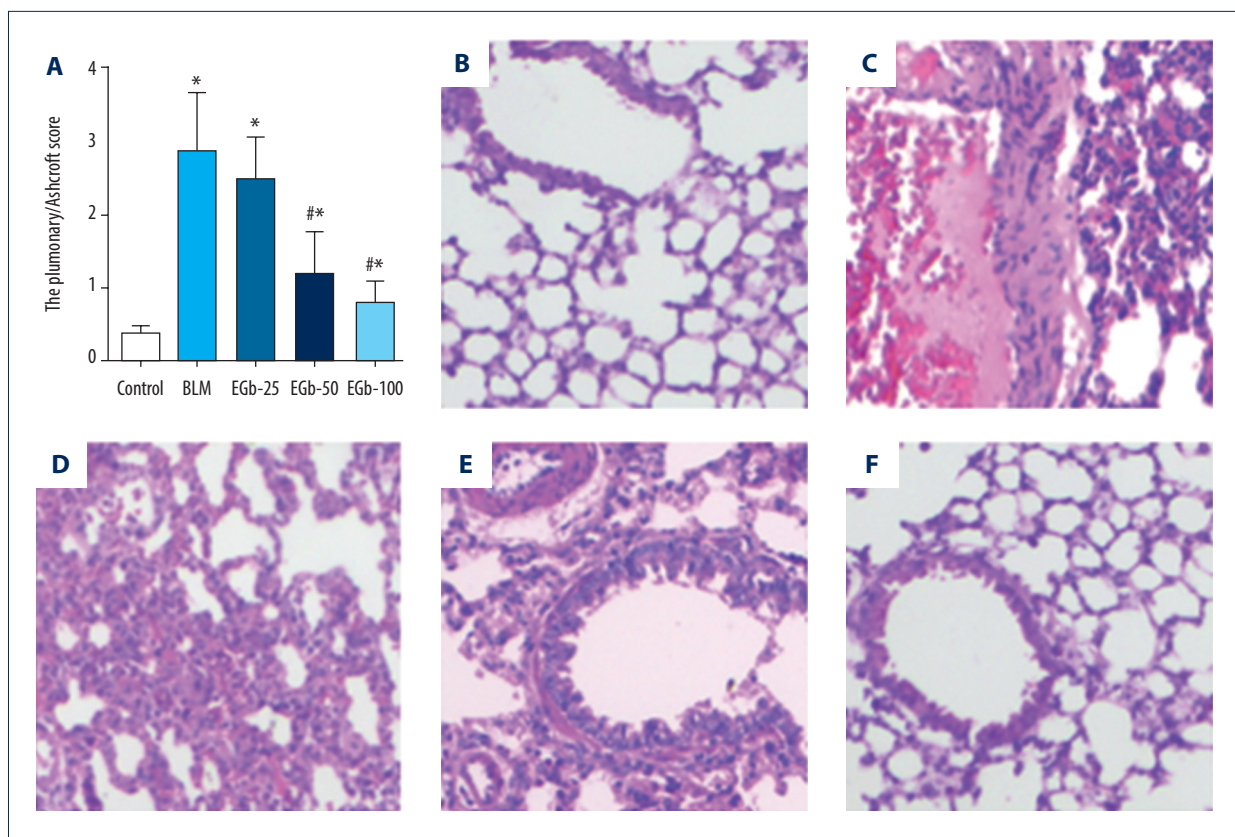


Figure 1. EGb761 suppresses pulmonary inflammation induced by bleomycin (BLM) in mice. (A) Pulmonary inflammation of mice was evaluated by lung alveolitis score after treatment with BLM for 28 days. Lung tissues from normal mice (B), BLM-treated group (C), low-dose EGb761 group (D), mild-dose EGb761 group (E), and high-dose EGb761 group (F) were stained with hematoxylin and eosin; magnifications were 200 \times . All data are shown as mean \pm standard deviation ($n=5$). * $P<0.05$ vs. normal group; # $P<0.05$ vs. BLM group.

were observed in the BLM-treated group by Masson staining (Figure 2B, 2C). EGb761 treatment, however, diminished the deposition of collagen (Figure 2D–2F). Furthermore, the proinflammatory cytokine level in serum on day 7, including TNF- α , IL-1 β , and IL-6, were evaluated by ELISA (Figure 3A–3C). The level of proinflammatory cytokines was increased by BLM treatment. Conversely, EGb-761 suppressed the cytokines.

EGb761 regulates the balance of M1/M2 macrophages and the expression of inflammation-associated proteins to prevent PF

Previous studies report that the pathogenesis of PF is related to immunology, and the balance between M1 and M2 macrophages has been a hot spot in PF pathogenesis. Regulation of the balance might be an important therapy to prevent PF. Therefore, the status of M1 and M2 macrophages in lung tissues was assessed by evaluating the levels of two types macrophage markers, inducible nitric oxide synthase and IL-10, respectively. Because of severe damage in lung tissue of the mice, enough pulmonary macrophages could not be obtained

for detection. Therefore, RT-PCR, another common method, was used instead of flow cytometry to detect the M1/M2 macrophages. The results showed that the M1 macrophages were decreased by BLM compared with the normal group; the M2 macrophages increased. However, after EGb761 treatment, macrophage levels returned to normal (Figure 4A). The ratio of the two types macrophages showed similar results (Figure 4B). In addition, the expression level of α -smooth muscle actin (SMA), the marker of myofibroblasts, was assessed by western blotting (Figure 4C). The expression of α -SMA was significantly increased by treatment with BLM compared with the normal group. However, treatment with EGb761 could suppress the increase in α -SMA expression. Meanwhile, the expression of TGF- β 1, which plays a role in the mechanism of macrophage-mediated PF, was assessed on day 28 after exposure to BLM and EGb761. The results showed that TGF- β 1 was increased by treating with BLM but was reduced by EGb761 (Figure 4D).

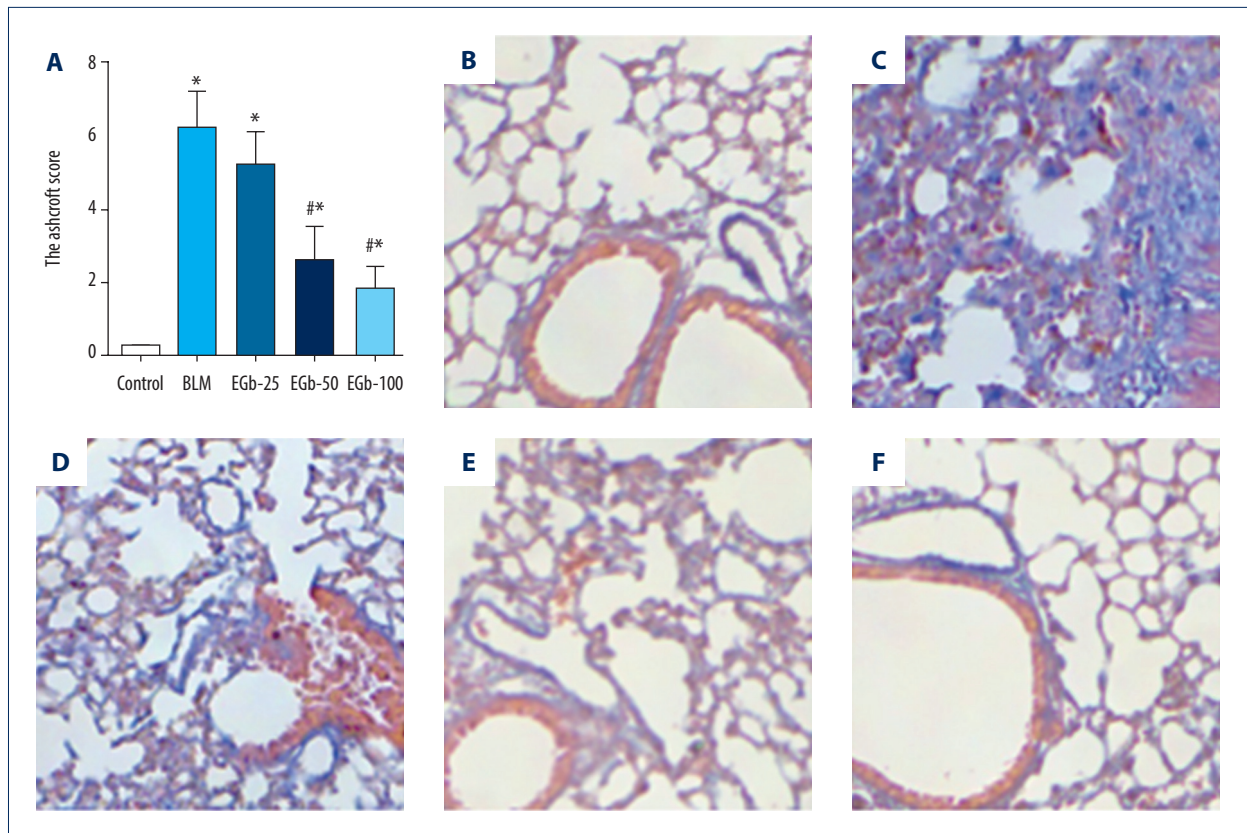


Figure 2. EGb761 protects mice from pulmonary fibrosis induced by bleomycin (BLM). (A) Protective effects of EGb761 on lung fibrosis induced by BLM were evaluated by Ashcroft score. Lung tissues from normal mice (B), BLM-treated group (C), low-dose EGb761 group (D), mild-dose EGb761 group (E), and high-dose EGb761 group (F) were stained with Masson stain; magnifications were 200 \times . All data are shown as mean \pm standard deviation ($n=5$). * $P<0.05$ vs. normal group; # $P<0.05$ vs. BLM group.

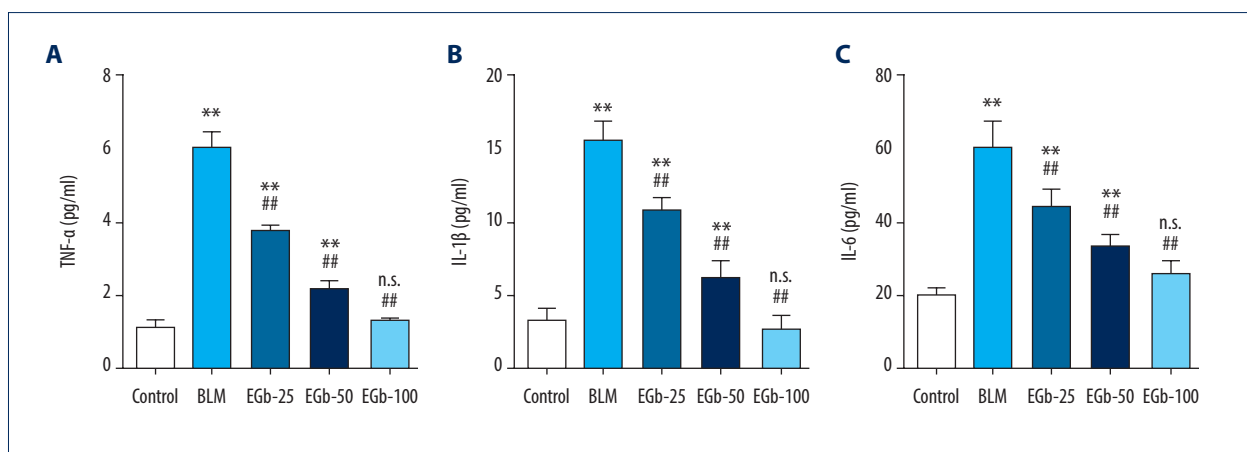


Figure 3. EGb761 suppresses bleomycin (BLM)-induced proinflammatory cytokines in the early stage. Mouse peripheral blood was collected on day 7 after BLM treatment. Levels of proinflammatory cytokines in serum, including tumor necrosis (TNF)- α (A), interleukin (IL)-1 β (B), and IL-6 (C), were detected by enzyme-linked immunosorbent assay kit. All data are shown as mean \pm standard deviation ($n=5$). ** $P<0.0001$ vs. normal group; ## $P<0.0001$ vs. BLM group.

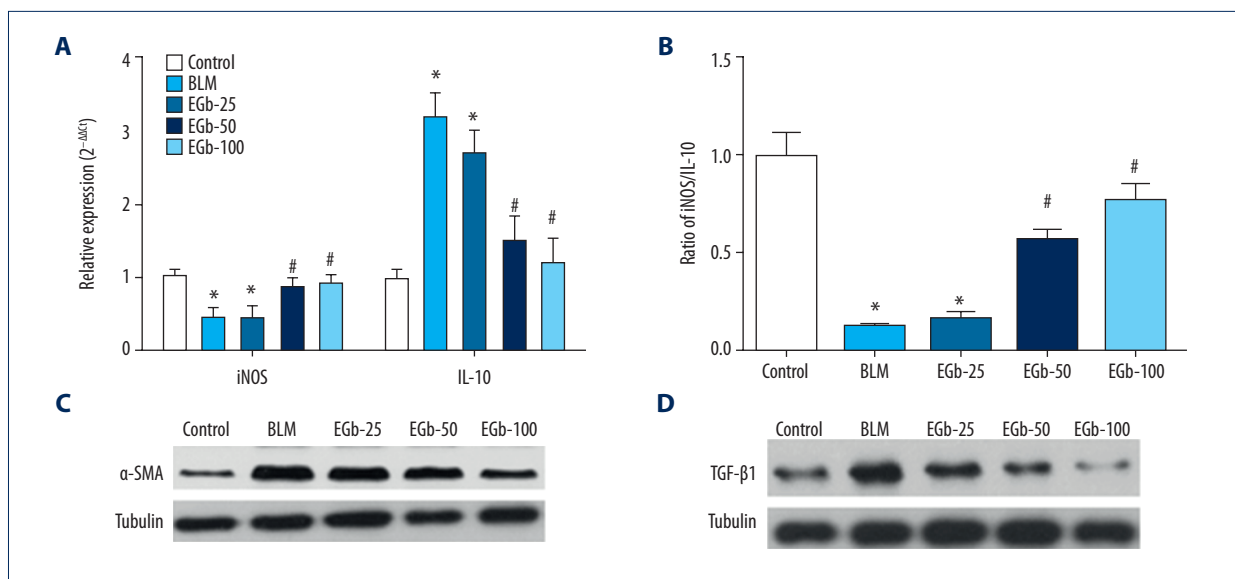


Figure 4. EGb761 regulates the balance of M1/M2 macrophages and expression of inflammation-associated proteins to prevent pulmonary fibrosis (PF). **(A)** Messenger ribonucleic acid (mRNA) expression levels of M1 (inducible nitric oxide synthase [iNOS]) and M2 (interleukin [IL]-10) macrophage markers in PF lung tissues were confirmed by real-time polymerase chain reaction. Glyceraldehyde 3-phosphate dehydrogenase (GAPDH) and tubulin served as a reference control and a loading control, respectively. **(B)** Ratio of M1 and M2 macrophages in lung tissues was calculated on the basis of the mRNA expression of iNOS and IL-10. The expression level of α -smooth muscle actin (SMA) **(C)** and transforming growth factor (TGF)- β 1 **(D)** in lung tissues was determined on day 28 after treating with BLM or EGb761 by western blotting. * $P < 0.05$ vs. normal group; # $P < 0.05$ vs. BLM group.

Egb761 reduced PF by regulating apoptosis factors in mouse PF model

Nuclear factor (NF)- κ B (p65)-mediated cellular apoptosis is considered one of the important factors in PF [40, 41]. First, the level of phosphorylated NF- κ B (p65) was evaluated by western blot. The result showed that the level of phosphorylated NF- κ B (p65) was induced by BLM on day 28, but was suppressed by treating with EGb761 (Figure 5A). Furthermore, the protective effects of EGb761 on lung cell apoptosis were investigated by evaluating the mRNA and protein levels of apoptosis factors including Bax, Bcl-2, caspase-3, and caspase-9 (Figure 5B, 5C). The results showed that treating with BLM significantly decreased the mRNA and protein levels of Bax and Bcl-2, whereas it increased caspase-3 and caspase-9 expression. Expression levels of all these factors returned to normal levels after treatment with EGb761 except for caspase-9.

Discussion

PF is a progressive and fatal disease with increasing annual incidence; there are few effective drugs approved for PF treatment [42]. In addition, the pathogenic mechanism of PF remains unknown. Previous studies indicated that EGb761 had a positive effect on BLM-induced PF in rats [43]. In this study, we showed the therapeutic potential of EGb761 in mice. The

results provided sufficient evidence suggesting that EGb761 treatment effectively reduced lung inflammation and PF in the induced (by BLM) PF mouse model.

PF showed pathological characteristics of the irreversible destruction and remodeling of lung tissues due to oversecretion of collagen and ECM components. The previous studies suggest that part of the reason was that the imbalance between M1 and M2 macrophage action induced abnormal reparation of lung tissues [44–46]. This imbalance changed the secretion of antifibrotic cytokines and profibrotic mediators by two types of macrophages to induce fibroproliferative tissue remodeling. In addition, the macrophage overactivation was observed in the wound-healing phase of the lung tissue after BLM, asbestos, radiation, or other materials treatment [47–51]. Increasing numbers of M2 macrophages were confirmed in the fibrotic tissue, which directly correlated with a worsening prognosis. The M2 macrophage was shown to be the major source of key profibrotic mediators, including TGF- β 1 [52,53]. In another study, the amount of M1 macrophage was upregulated in the M2 macrophage-suppressed animal model with reduced fibrosis, which means that the balance in activity of the two types of macrophages affects the outcome of the response to fibrotic stimulation. In this study, M1 and M2 macrophages lost that balance after treatment with BLM in the mouse model, as well as in previous studies. Nevertheless, EGb761 restored the balance, suggesting that the potential

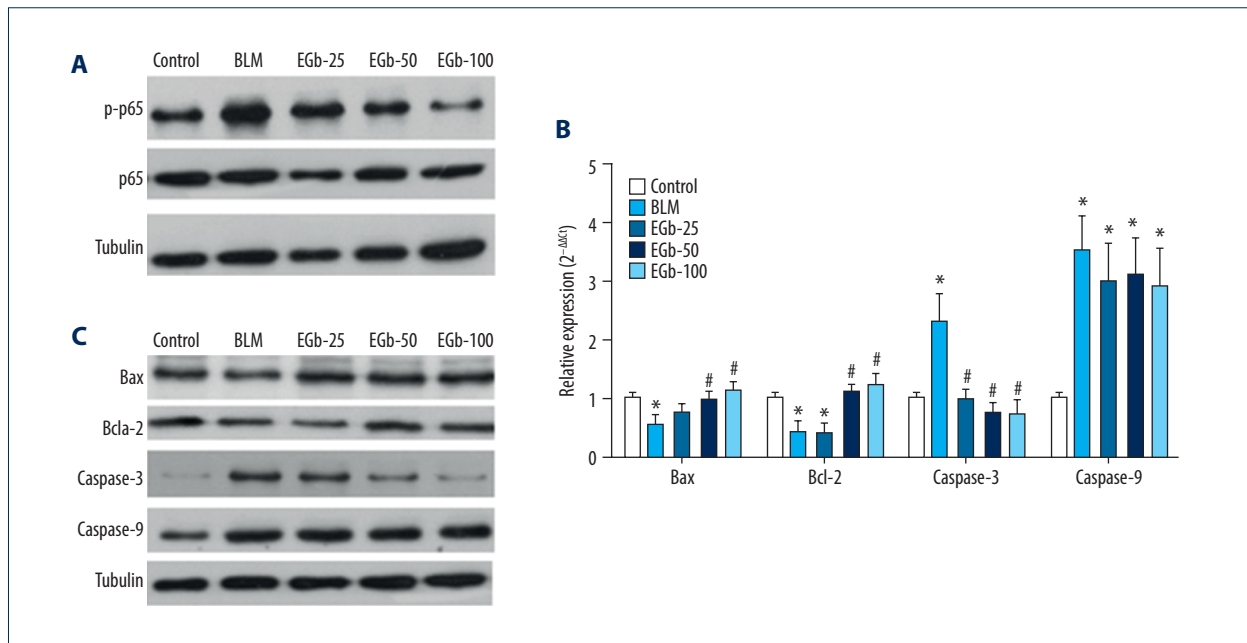


Figure 5. EGb761 reduced pulmonary fibrosis (PF) by regulating apoptosis factors in mouse PF model after treating with bleomycin (BLM) or EGb761 for 28 days. **(A)** Expressions of phosphorylated nuclear factor (NF)- κ B (p65) were validated by western blot. The messenger ribonucleic acid and protein levels of apoptosis factors including B-cell lymphoma X protein (Bax), B-cell lymphoma (Bcl)-2, caspase-3, and caspase-9 in lung tissues of mice from each group were validated by real-time polymerase chain reaction **(B)** and western blotting **(C)**. Glycerinaldehyde 3-phosphate (GAPDH) and tubulin served as the reference control and loading control, respectively. * $P < 0.05$ vs. normal group; # $P < 0.05$ vs. BLM group.

mechanisms of therapeutic effects of EGb761 might be attributed to regulation of the balance between M1 and M2 macrophages and the related pulmonary inflammation.

Furthermore, several studies showed that the AECs were sensitive to apoptosis in injured lung tissue, which was the key incident in PF [21–24,54,55]. The NF- κ B pathway was considered to be related to excessive apoptosis of AECs in PF [56,57]. The apoptosis of AECs caused by persistent irritants contributes not only to activating the resident fibroblasts to proliferate for repairing injury of the lung tissue, but also to recruiting the inflammatory cells as well as macrophages, which then induce the excessive deposition of scars in lung tissues [17,58,59]. The results of this study showed that the level of caspase-3 was upregulated, whereas the levels of Bax and Bcl-2 were downregulated with the increasing amount of phosphorylated NF- κ B after BLM treatment. However, the levels of these

substances were restored by EGb761 treatment, suggesting that EGb761 resisted PF by suppressing the NF- κ B-mediated cellular apoptosis.

Conclusions

Our study used the mouse model to reveal the potential clinical therapeutic effect of EGb761 on BLM-induced PF from multiple perspectives by regulating the balance of M1/M2 macrophages and suppressing the NF- κ B-mediated apoptosis of AECs. This study provided a novel possibility for the curability of PF.

Conflict of interest

None.

References:

- Fernandez IE, Eickelberg O: New cellular and molecular mechanisms of lung injury and fibrosis in idiopathic pulmonary fibrosis. *Lancet*, 2012; 380: 680–88
- Newton CA, Zhang D, Oldham JM et al: Telomere length and use of immunosuppressive medications in idiopathic pulmonary fibrosis. *Am J Respir Crit Care Med*, 2018; 47: 1141–51
- Collard HR, Chen SY, Yeh WS et al: Health care utilization and costs of idiopathic pulmonary fibrosis in U.S. Medicare beneficiaries aged 65 years and older. *Ann Am Thorac Soc*, 2015; 12: 981–87
- Collard HR, Ward AJ, Lanes S et al: Burden of illness in idiopathic pulmonary fibrosis. *J Med Econ*, 2012; 15: 829–35
- Torrisi SE, Ley B, Kreuter M et al: The added value of comorbidities in predicting survival in idiopathic pulmonary fibrosis: A multicentre observational study. *Eur Respir J*, 2019; 53: 1801587
- Chilosi M, Caliò A, Rossi A et al: Epithelial to mesenchymal transition-related proteins ZEB1, β -catenin, and β -tubulin-III in idiopathic pulmonary fibrosis. *Mod Pathol*, 2017; 30: 26–38
- Zuo F, Kaminski N, Eugui E et al: Gene expression analysis reveals matrixin as a key regulator of pulmonary fibrosis in mice and humans. *Proc Natl Acad Sci USA*, 2002; 99: 6292–97
- Jiang D, Liang J, Fan J, Yu S et al: Regulation of lung injury and repair by toll-like receptors and hyaluronan. *Nat Med*, 2005; 11: 1173–79
- Song E, Ouyang N, Hörbelt M et al: Influence of alternatively and classically activated macrophages on fibrogenic activities of human fibroblasts. *Cell Immunol*, 2000; 204: 19–28
- Takeuchi O, Akira S: Pattern recognition receptors and inflammation. *Cell*, 2010; 140: 805–20
- Gordon S, Martinez FO: Alternative activation of macrophages: Mechanism and functions. *Immunity*, 2010; 32: 593–604
- Pechkovsky DV, Prasse A, Kollert F et al: Alternatively activated alveolar macrophages in pulmonary fibrosis – mediator production and intracellular signal transduction. *Clin Immunol*, 2010; 137: 89–101
- Venosa A, Malaviya R, Choi H et al: Characterization of distinct macrophage subpopulations during nitrogen mustard-induced lung injury and fibrosis. *Am J Respir Cell Mol Biol*, 2016; 54: 436–46
- He C, Murthy S, McCormick ML et al: Mitochondrial Cu, Zn-superoxide dismutase mediates pulmonary fibrosis by augmenting H₂O₂ generation. *J Biol Chem*, 2011; 286: 15597–607
- Jain M, Rivera S, Monclus EA et al: Mitochondrial reactive oxygen species regulate transforming growth factor- β signaling. *J Biol Chem*, 2013; 288: 770–77
- Osborn-Heaford HL, Ryan AJ, Murthy S et al: Mitochondrial Rac1 GTPase import and electron transfer from cytochrome c are required for pulmonary fibrosis. *J Biol Chem*, 2012; 287: 3301–12
- Kage H, Borok Z: EMT and interstitial lung disease: A mysterious relationship. *Curr Opin Pulm Med*, 2012; 18(5): 517–23
- King TE Jr., Pardo A, Selman M: Idiopathic pulmonary fibrosis. *Lancet*, 2011; 378: 1949–61
- Drakopanagiotakis F, Xifteri A, Polychronopoulos V, Bouros D: Apoptosis in lung injury and fibrosis. *Eur Respir J* 2008; 32: 1631–38
- Konishi K, Gibson KF, Lindell KO et al: Gene expression profiles of acute exacerbations of idiopathic pulmonary fibrosis. *Am J Respir Crit Care Med*, 2009; 180: 167–75
- Plataki M, Koutsopoulos AV, Darivianaki K et al: Expression of apoptotic and antiapoptotic markers in epithelial cells in idiopathic pulmonary fibrosis. *Chest*, 2005; 127: 266–74
- Cheresh P, Kim SJ, Tulasiram S, Kamp DW: Oxidative stress and pulmonary fibrosis. *Biochim Biophys Acta*, 2013; 1832: 1028–40
- Cui Y, Robertson J, Maharaj S et al: Oxidative stress contributes to the induction and persistence of TGF- β 1 induced pulmonary fibrosis. *Int J Biochem Cell Biol*, 2011; 43: 1122–33
- Lekkerkerker AN, Aarbiou J, van Es T, Janssen RA: Cellular players in lung fibrosis. *Curr Pharm Des*, 2012; 18: 4093–102
- Milara J, Ballester B, Morell A et al: JAK2 mediates lung fibrosis, pulmonary vascular remodelling and hypertension in idiopathic pulmonary fibrosis: An experimental study. *Thorax*, 2018; 73: 519–29
- Le TT, Karmouty-Quintana H, Melicoff E et al: Blockade of IL-6 trans signaling attenuates pulmonary fibrosis. *J Immunol*, 2014; 193: 3755–68
- Zhao J, Ren Y, Qu Y et al: Pharmacodynamic and pharmacokinetic assessment of pulmonary rehabilitation mixture for the treatment of pulmonary fibrosis. *Sci Rep*, 2017; 7: 3458
- Tulsulkar J, Glueck B, Hinds TD, Shah ZA: *Ginkgo biloba* extract prevents female mice from ischemic brain damage and the mechanism is independent of the HO1/Wnt pathway. *Transl Stroke Res*, 2016; 7: 120–31
- Dodge HH, Zitzelberger T, Oken BS et al: A randomized placebo-controlled trial of *Ginkgo biloba* for the prevention of cognitive decline. *Neurology*, 2008; 70: 1809–17
- Chen L, Zhang C, Han Y et al: *Ginkgo biloba* extract (EgB) inhibits oxidative stress in neuro 2A cells overexpressing APPsw. *Biomed Res Int*, 2019; 2019: 7034983
- Pan C, Liu N, Zhang P et al: EGb761 ameliorates neuronal apoptosis and promotes angiogenesis in experimental intracerebral hemorrhage via RSK1/GSK3 β pathway. *Mol Neurobiol*, 2018; 55(2): 1556–67
- Wan W, Zhang C, Danielsen M et al: EGb761 improves cognitive function and regulates inflammatory responses in the APP/PS1 mouse. *Exp Gerontol*, 2016; 81: 92–100
- Shamskhou EA, Kratochvil MJ, Orcholski ME et al: Hydrogel-based delivery of IL-10 improves treatment of bleomycin-induced lung fibrosis in mice. *Biomaterials*, 2019; 203: 52–62
- Zhang QS, Wang XP, Liu H et al: [Protective effect of *Ginkgo biloba* extract on paracetamol-induced acute hepatic injury in mice.] *Zhongguo Ying Yong Sheng Li Xue Za Zhi*, 2018; 34(5): 432–35, 469 [in Chinese]
- McKeage K, Lyseng-Williamson KA: *Ginkgo biloba* extract Egb 761® in the symptomatic treatment of mild-to-moderate dementia: A profile of its use. *Drugs Ther Perspect*, 2018; 34(8): 358–66
- Czauderna C, Palestino-Dominguez M, Jens U et al: *Ginkgo biloba* induces different gene expression signatures and oncogenic pathways in malignant and non-malignant cells of the liver. *PLoS One*, 2018; 13(12): e0209067
- Biddlestone L, Corbett AD, Dolan S: Oral administration of *Ginkgo biloba* extract, EGb-761 inhibits thermal hyperalgesia in rodent models of inflammatory and post-surgical pain. *Br J Pharmacol*, 2007; 151(2): 285–91
- Zhang J, Cui R, Feng Y et al: Serotonin exhibits accelerated bleomycin-induced pulmonary fibrosis through TPH1 knockout mouse experiments. *Mediators Inflamm*, 2018; 2018: 7967868
- Dubin PJ, McAllister F, Kolls JK: Is cystic fibrosis a TH17 disease? *Inflamm Res*, 2007; 56: 221–27
- Chen S, Cui G, Peng C et al: Transplantation of adipose-derived mesenchymal stem cells attenuates pulmonary fibrosis of silicosis via anti-inflammatory and anti-apoptosis effects in rats. *Stem Cell Res Ther*, 2018; 9: 110.
- Ayub EA, Kolb PS, Mohammed-Ali Z et al: GRP78 and CHOP modulate macrophage apoptosis and the development of bleomycin-induced pulmonary fibrosis. *J Pathol*, 2016; 239: 411–25
- Karimi-Shah BA, Chowdhury BA: Forced vital capacity in idiopathic pulmonary fibrosis – FDA review of pirfenidone and nintedanib. *N Engl J Med*, 2015; 372: 1189–91
- Daba MH, Abdel-Aziz AA, Moustafa AM et al: Effects of l-carnitine and ginkgo biloba extract (EGb 761) in experimental bleomycin-induced lung fibrosis. *Pharmacol Res*, 2002; 45: 461–67
- Alber A, Howie SE, Wallace WA, Hirani N: The role of macrophages in healing the wounded lung. *Int J Exp Pathol*, 2012; 93: 243–51
- Byrne AJ, Maher TM, Lloyd CM: Pulmonary macrophages: A new therapeutic pathway in fibrosing lung disease? *Trends Mol Med*, 2016; 22: 303–16
- Herold S, Mayer K, Lohmeyer J: Acute lung injury: How macrophages orchestrate resolution of inflammation and tissue repair. *Front Immunol*, 2011; 2: 65
- Huang Y, Zhang W, Yu F, Gao F: The cellular and molecular mechanism of radiation-induced lung injury. *Med Sci Monit*, 2017; 23: 3446–50
- Duke KS, Bonner JC: Mechanisms of carbon nanotube-induced pulmonary fibrosis: A physicochemical characteristic perspective. *Wiley Interdiscip Rev Nanomed Nanobiotechnol*, 2018; 10: e1498
- Laskin DL, Sunil VR, Gardner CR, Laskin JD: Macrophages and tissue injury: Agents of defense or destruction? *Annu Rev Pharmacol Toxicol*, 2011; 51: 267–88

50. Malaviya R, Gow AJ, Francis M et al: Radiation-induced lung injury and inflammation in mice: Role of inducible nitric oxide synthase and surfactant protein D. *Toxicol Sci*, 2015; 144: 27–38
51. Murthy S, Larson-Casey JL, Ryan AJ et al: Alternative activation of macrophages and pulmonary fibrosis are modulated by scavenger receptor, macrophage receptor with collagenous structure. *FASEB J*, 2015; 29: 3527–36
52. Pulichino A-M, Wang I-M, Caron A et al: Identification of transforming growth factor β 1-driven genetic programs of acute lung fibrosis. *Am J Respir Cell Mol Biol*, 2008; 39: 324–36
53. Shvedova AA, Kisin ER, Mercer R et al: Unusual inflammatory and fibrogenic pulmonary responses to single-walled carbon nanotubes in mice. *Am J Physiol Lung Cell Mol Physiol*, 2005; 289: L698–708
54. Gunther A, Lubke N, Ermert M et al: Prevention of bleomycin-induced lung fibrosis by aerosolization of heparin or urokinase in rabbits. *Am J Respir Crit Care Med*, 2003; 168: 1358–65
55. Kuwano K: Involvement of epithelial cell apoptosis in interstitial lung diseases. *Intern Med*, 2008; 47: 345–53
56. Im J, Kim K, Hergert P, Nho RS: Idiopathic pulmonary fibrosis fibroblasts become resistant to Fas ligand-dependent apoptosis via the alteration of decoy receptor 3. *J Pathol*, 2016; 240: 25–37
57. Wu Q, Zhou Y, Zhou XM: Citrus alkaline extract delayed the progression of pulmonary fibrosis by inhibiting p38/NF- β signaling pathway-induced cell apoptosis. *Evid Based Complement Alternat Med*, 2019; 2019: 1528586
58. Wynn TA, Ramalingam TR: Mechanisms of fibrosis: Therapeutic translation for fibrotic disease. *Nat Med*, 2012; 18: 1028–40
59. Kim KK, Kugler MC, Wolters PJ et al: Alveolar epithelial cell mesenchymal transition develops *in vivo* during pulmonary fibrosis and is regulated by the extracellular matrix. *Proc Natl Acad Sci USA*, 2006; 103: 13180–85